SUPPORTING MATERIALS AND METHODS

Experimental methods

Adaptation protocol

One way to assess the submodality composition of a neuron is to measure its response to a skin indentation (1). Indeed, SA1 fibers are the only ones to respond during the sustained portion of the indentation whereas RA and PC fibers are the only ones to respond during the offset of the indentation. To the extent that a cortical neuron exhibits both of these properties, we can infer that it receives convergent input from multiple classes of tactile fibers. With this in mind, we measured the response of cortical neurons to a probe indented into the skin. Specifically, we indented the drum-mounted load cell (a cylinder of diameter 7 mm, see above) vertically into the skin to the 15 g reference point, and held the indentation for 500 ms, before removing it from the skin (5 mm/s indentation/removal speed). This indentation was repeated 60 times, with an inter-trial interval of 500 ms. We completed this protocol for 94 neurons (28, 57, and 9 from areas 3b, 1, and 2, respectively).

Spatial receptive fields

To systematically measure the spatial receptive field of individual cortical neurons, we designed a 3D-printed random dot array following a previously described approach (2) (truncated cones: 0.5 mm dot height, 1 mm base diameter, 0.5 mm top diameter, 10 dots/cm^2, dots uniformly distributed, 5 cm x 16 cm). The random dot pattern was scanned over the skin 100 times but, after each scan, the drum was stepped 400 microns along its axis of rotation. A full uninterrupted protocol was completed (~10 minutes), for 72 neurons (27, 37, and 8 from areas 3b, 1, and 2, respectively).

Analysis

Adaptation index

For data from the indented probe protocol, we measured the trial-by-trial firing rate over stimulus epochs: 1) background activity, measured between 1 s and 500 ms before the probe was indented into the skin, 2) sustained response activity, measured during the 500 ms hold period, and 3) offset response activity, measured between 100 and 300 ms after the probe started lifting off the skin. We report that a neuron has a significant sustained/offset response if its texture elicited firing rate was significantly different from baseline (two-sided t-test for sustained/offset-baseline, significant if p<0.05). To quantify the relative magnitude of the sustained and offset responses, we calculated the fraction of the combined sustained and offset responses that was carried by the offset response:

$$f_o = \frac{|r_o - r_b|}{|r_o - r_b| + |r_s - r_b|}$$

where r_o is the firing rate at the offset, r_s is the firing rate during the sustained phase, and r_b is the baseline firing rate.

Binary classification and dimensionality

The dimensionality of the cortical population response estimated from PCA comprises components that reliably carry texture information and components that do not. To estimate the components of the dimensionality that contribute to the texture representation, we adapted a method from (3) that

www.pnas.org/cgi/doi/10.1073/pnas.1818501116116

assesses the number of informative dimensions by quantifying the ability of the population representation to perform arbitrary linear binary classifications of the state space (in this case textures). The idea is, to the extent that the texture set can be arbitrarily split into *D* categories, the neural space comprises *D* dimensions relevant to texture coding. First, we randomly select N neurons and T textures. We choose one (of the 2^T possible ways) of splitting the T textures into two groups, and test whether a binary classifier could successfully discriminate between the two groups using the N-dimensional population response. Specifically, we train a support vector machine with a linear kernel (with the *fitcsvm()* function in Matlab) on four randomly selected responses to each texture (out of five, without replacement), each yielding an N-dimensional vector of firing rates. We then use the remaining left-out response from each cell to build a single N-dimensional test vector for each texture, which is used to test the performance of the binary classifier. Performance is averaged over 50 repetitions of the trial-shuffling procedure, to get a mean performance for this set of cells and texture groups. If this mean performance is greater than 75%, we count this binary classification as "implementable" by the population response. The functions in Fig. 3B represent the proportion of "implementable" conditions, measured over 500 random selections of cells and texture groupings. Data are fit with sigmoids:

$$p(T) = \exp(-(T/\beta)^{\alpha})$$

and the intersection of this curve *p(T)* = 0.95 is taken as the critical value T* for each population size. A population that can successfully classify T* textures has an effective dimensionality of T*-1. Thus, in Fig. 3C, we report the dimensionality for a population size N as *D = max(T*-1, 0)*.

This method of measuring dimensionality provides a lower bound on the true dimensionality of the neural representation (3). To verify this, we generated representations of texture with an imposed dimensionality (by projecting the neuronal response onto a subset of principal components), and then measured the dimensionality of these new texture responses using the binary classification metric (see SI Appendix, Fig. S2E-I). Specifically, to create an N-dimensional space of texture responses, we constructed new responses by deriving each neuron's mean firing rate from the first N principal components. To obtain single trial responses, we subtracted the raw mean firing rate for each texture from each single-trial response and added the corresponding mean reconstructed from the lower-dimensional representation. Thus, the trial-to-trial variability in the responses of individual neurons to individual textures was preserved, but the dimensionality of the population response was reduced to N.

Simulating noise correlations

We sought to test the impact on texture classification and neural dimensionality of noise correlations – absent from neuronal responses because they were measured non-simultaneously – by simulating the effects of noise correlations using a resampling technique. First, for each texture, we generated a set of 5 population response vectors (across all 141 cells) using data from its 5 repeated presentations. These repetitions were ordered from highest to lowest firing rate, such that the first population vector contained the highest firing rate response for each individual cell, the second vector contained the second highest rate response, etc. Repeating this procedure across all textures created a set of population vectors (5x59) with a very high level of mean noise correlation (r_{sc}=0.74). To bring this value to physiologically relevant levels (r_{sc}=0.1-0.2, cf. ref. (4)), we repeatedly looped over each cell/texture combination (10 times) and randomly swapped two of the repetitions between population vectors with a set probability (p = 0.15, 0.2, 0.26 and 0.8). This resulted in sets of population vectors with physiologically relevant levels of mean noise correlation (r_{sc}=0.22, 0.14, 0.08 and 0.001, respectively).

To perform our texture classification with these resampled neuronal responses, we repeated the classification procedure described above with only one difference: performance was only calculated using each of the 5 population vectors with targeted correlations as the "single trial response," rather than using randomly selected responses on each shuffle. When applicable, responses were still averaged over 100 randomly selected groups of cells at each group size. We also recalculated our dimensionality analyses using these resampled data sets. Rather than using the random shuffling procedure, we iterated over each of the 5 simulated population vectors as the "left out response." Each point in SI Appendix, Fig. S2G represents the mean number of "implementable" texture sets, averaged over 300 random texture groupings.

Spatial receptive fields

To characterize the spatial receptive field of each cortical neuron, we adopted an approach described in detail in ref. (2). In brief, we first binned spiking responses to the receptive field protocol (see above) in 100-micron (1.25 ms) bins. The 100 runs – each corresponding to the response during one scan of the random dot pattern, each scan radially displaced from the previous one by 400 microns – were combined into a neural image (spatial even plot, cf. ref. (5)), which was then cross-correlated with a reconstruction of the stimulus (binned into 100x100 micron bins) to find an optimal alignment. Then, we used a spike-triggered average (STA) of the stimulus to find the mean stimulus values that were spatially aligned to any given spike.

To calculate receptive field properties, we first smoothed the STA with a 0.3 mm std. dev. Gaussian filter. Next, all bins with an absolute amplitude less than 20% of the RF's peak amplitude were set to zero. Finally, we required 1) that every non-zero bin have at least two of the four adjacent bins be nonzero and 2) that isolated regions of the RF have areas of at least 0.7 mm^2. Bins that did not meet these criteria were set to zero. To calculate excitatory & inhibitory area, we summed the area occupied by bins in the RF with positive/negative values, respectively. To calculate the scanning distance between excitatory and inhibitory subfields, we first found the center-of-mass for the excitatory and inhibitory bins in each RF, and then calculated the distance between them along the scanning direction.

SUPPORTING FIGURES

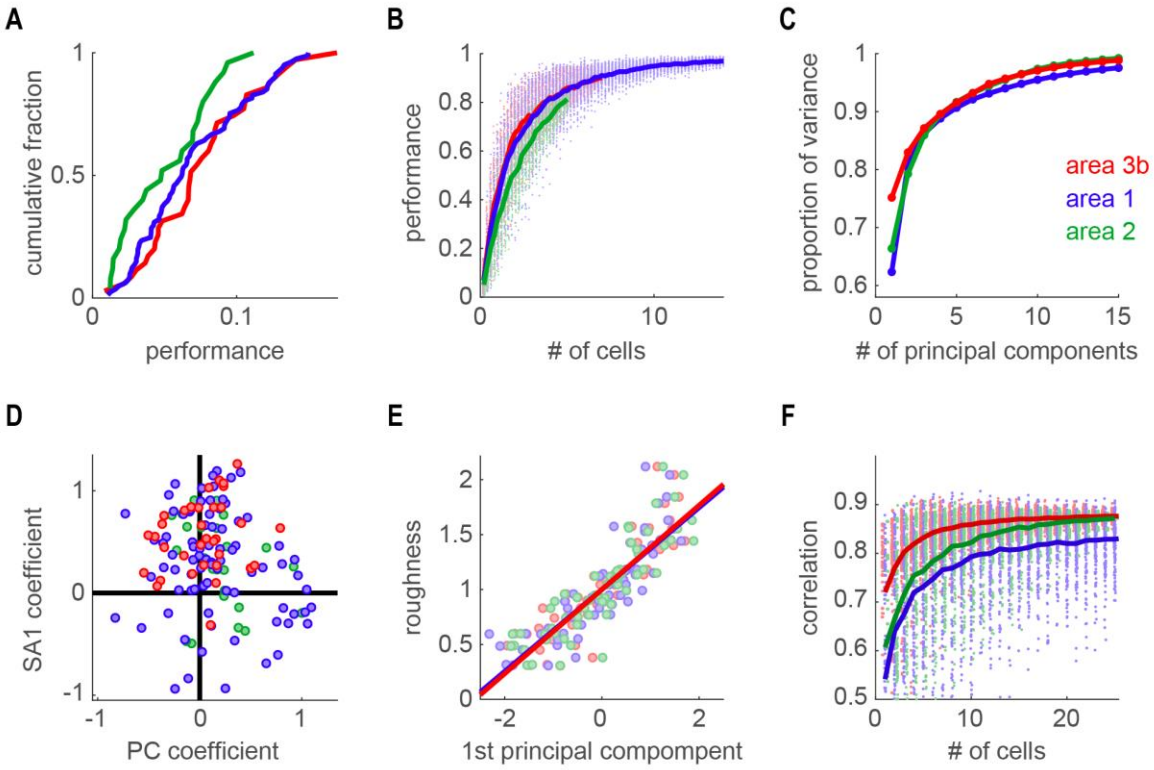

Figure S1. **Texture responses are similar across cortical fields.** A| Cumulative distribution of texture classification performance based on the responses of individual neurons for Brodmann's areas 3b, 1, and 2 (red, blue, and green, respectively). B| Texture classification performance of groups of neurons in each area as a function of group size (as in Figure 2). Each dot denotes a random sample, the line denotes the mean at each group size. Classification performance is largely similar across areas. C| Cumulative scree plot (proportion of variance explained) for the first 15 principal components within each cortical area. In all three areas, the bulk of the response variance is explained by only a few PCs. D| Normalized SA1 afferent regression coefficient vs. normalized PC afferent regression coefficient for each neuron in areas 3b (red), 1 (blue), and 2 (green) . Note that the most strongly PC-like neurons are located in areas 1 and 2. E| Perceived roughness of individual textures is plotted against the first principal component of cortical responses in area 3b (r=0.88, red), area 1 (r=0.86, blue), and area 2 (r=0.87, green). The best fit lines for all three areas lie on top of each other. F| Correlation between roughness and the first principal component vs. the number or cells included in the principal components analysis. Dots denote the performance of random samples of neurons, traces denote the mean within each area for each sample size.

s

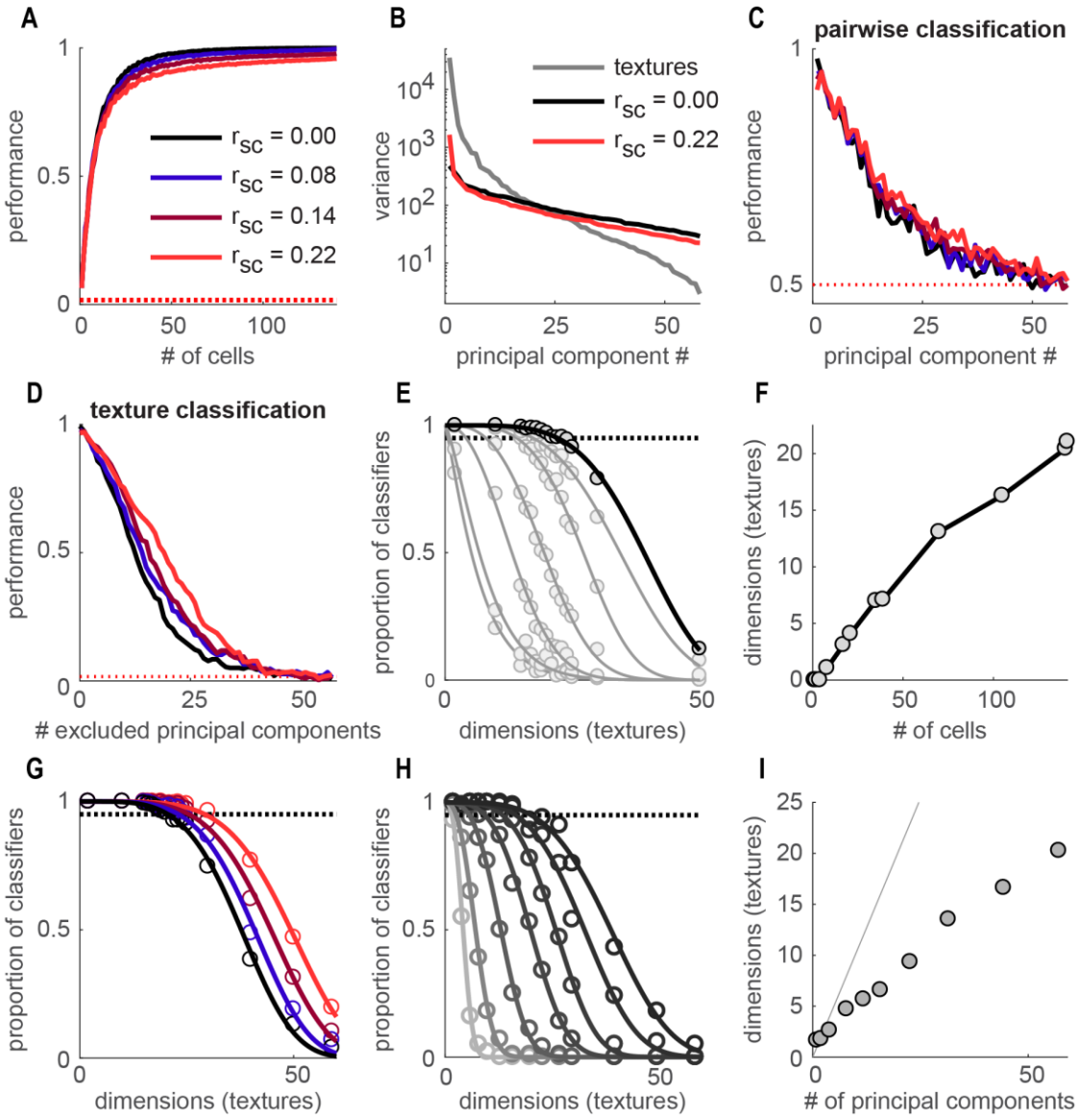

Figure S2. **Texture classification and dimensionality estimation are robust to noise correlations.** A| Texture classification performance vs. group size with varying levels of simulated noise correlations (r_{sc} ranging from 0.0 to 0.22, see Methods). Classification is relatively insensitive to noise correlation. B| Variance of each principal component (plotted in logarithmic units), shown for the cortical population response (in grey) and for the simulated noise in the low (black) and high (red) correlation cases. As mean noise correlations increase, noise variance shifts away from smaller principal components of the texture response, and onto the first principal component. As a result, these noise correlations lead to additional low-variance dimensions rising above the noise variance floor. C| Pairwise texture classification using individual principal components (as in Figure 3C) with simulated noise correlations. Again, classification is largely unaffected by noise correlations. D| Texture classification based on low-

variance subsets of the principal components (as in Figure 3D) with simulated noise correlations. The dimensionality of the texture representation increases as the level of noise correlation increases, consistent with the falling noise floor illustrated in Figure S3B. E| The fraction of implementable binary classifications vs. the number of textures included in the classification (plotted in black). We can split almost any collection of 22 textures (~95% of groups, dotted line) into two arbitrary groups and distinguish those groups (performance > 0.75) with a binary classifier. From this analysis, we estimate the population representation of texture (for these 141 cells) to be at least 21-dimensional. Results from the same analysis, performed on subsets of cells, are shown in shades of grey (from left to right, N=1, 2, 17, 35, 70, 105). F| Number of dimensions estimated from the binary classification analysis vs. the number of cells used in the analysis. Dimensionality is still rapidly rising with group size up to 141, suggesting that the population representation of texture is larger than 21-dimensional across the full cortical population. G| The fraction of implemented binary classifications vs. number of textures included in the analysis (as in Figure S3E) with simulated noise correlations. Consistent with Figure S3B, the dimensionality of the texture representation increases for as the level of noise correlation increases. H| Fraction of the number of implementable binary classifications vs. number of textures for different projections of the full subspace onto low-dimensional subspaces (N=2, 6, 10, 16, 20, 23, 27 principal components, ranging from light grey to black). In all cases, the measured dimensionality from the binary classification analysis acts as a lower bound on the true dimensionality of the neural space (consistent with (3)). I| Estimated dimensionality of the space vs. the true dimensionality of the generated subspace. Each point's location along the ordinate corresponds to the intersection of the fitted sigmoid curve with the 95% threshold. The grey line represents the unity slope. Every point lies below this line, illustrating that the dimensionality analysis underestimates the underlying dimensionality of the neural space.

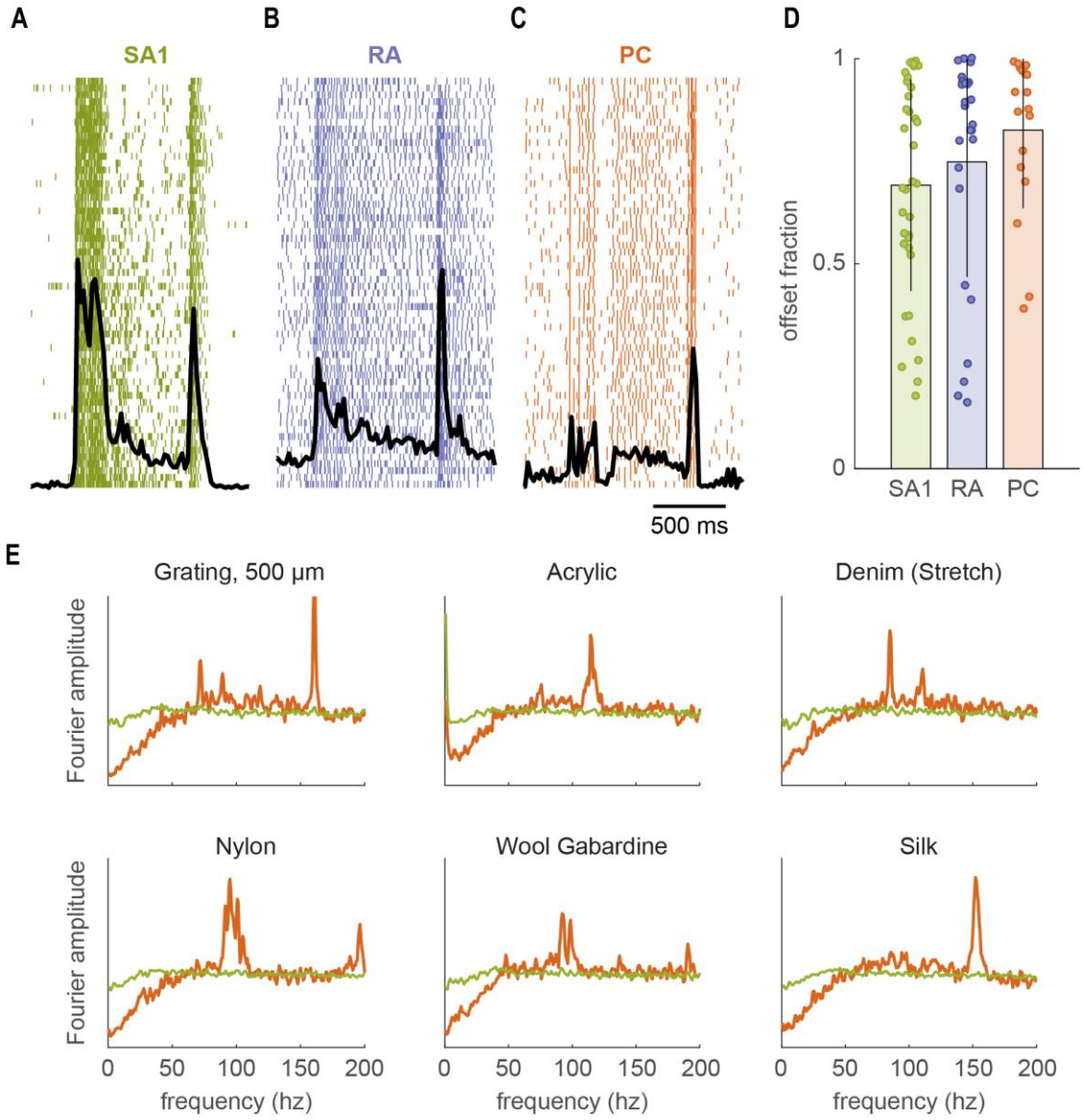

Figure S3. **Cortical neurons exhibit signatures of their afferent input.** A-C| Spiking responses of 3 different neurons to a probe indented into the skin for 500 ms (60 repetitions). Peri-stimulus time histograms of the spiking responses are shown in black. Many neurons which, according to the multiple regression, receive dominant input from SA1 (A), RA (B), or PC (C) fibers still exhibit both a sustained response and an off response, suggesting convergent input from the three classes of tactile fibers. D| Fraction of the combined sustained and offset response carried by the offset response for SA1-like (green, N=53), RA-like (blue, N=45), or PC-like (orange, N=23) neurons. Error bars denote the standard deviation of fractions across cells. While SA1 fibers exhibit no offset responses (1), most SA1-like neurons exhibit strong offset responses (p<0.05 for 93% of SA1-like neurons, paired-sample t-test). Similarly, while RA and PC fibers produce essentially no sustained response (1), many RA-like and PC-like neurons produce robust sustained responses (p<0.05 83%, and 68% of RA-like and PC-like neurons,

paired-sample t-test). Overall, 65/94 (69%) of neurons exhibited significant modulation in both their offset and sustained responses, and, of the remaining 29, ten yielded two or more significant weights in the multiple regression (*F*-test, as in the main text). Thus, in total, 75/94 (80%) neurons displayed submodality convergence by one or both of these measures. E| The mean absolute value of the Fourier transform of the spiking responses of SA1-like cells (green, cells with SA1 coefficient > 0.5, N=53) and PC-like cells (orange, cells with PC regression coefficient > 0.5, N=23) to six different textures. PC-like cells exhibit texture-evoked phase locking to frequencies between 50-200 Hz.

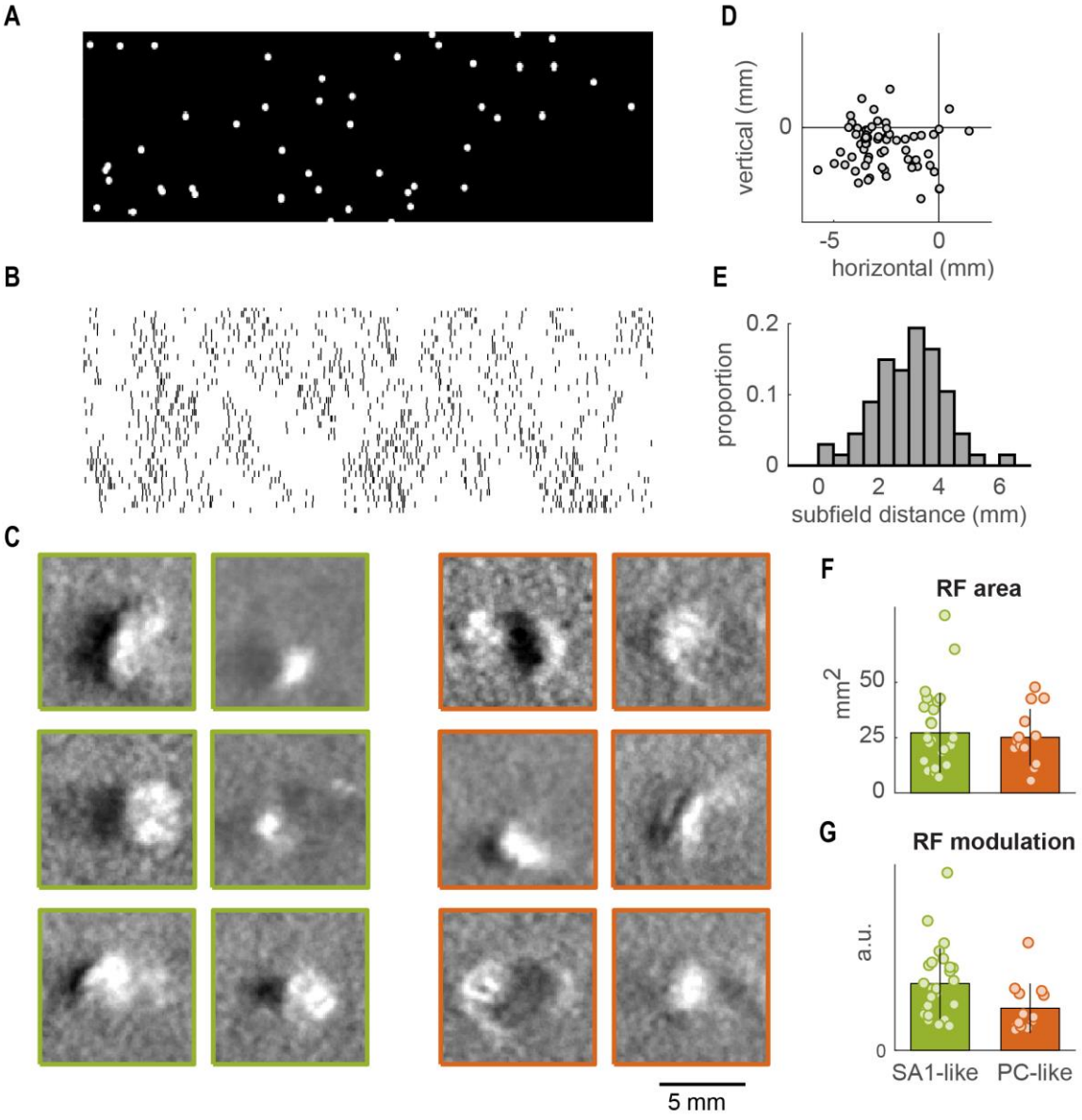

Figure S4. **Spatial receptive fields of somatosensory neurons.** A| Patch of the random dot pattern used to obtain spatial receptive fields. B| Spatial event plot of the spiking response of a cortical neuron to the stimulus patch. A spike-triggered average of the stimulus over this response was used to calculate a spatial receptive field. C| Example receptive fields from 12 example neurons: 6 are SA1-like (left, cells with SA1 coefficient > 0.5) and 6 are PC-like (right, cells with PC regression coefficient > 0.5, N=23). The top left RF was obtained from an SA1-like neuron whose response is shown in panel S4B. White regions are excitatory, black regions are inhibitory. D| Location of the inhibitory center relative to the excitatory center, for all of the measured spatial receptive fields (N=72). Inhibitory subfields were spatially offset from excitatory ones. Most inhibition is located behind the excitatory subfield horizontally (i.e., temporally lagged). E| Histogram of excitatory-inhibitory subfield distance across all measured cells. Inhibition was generally located 2-4 mm behind excitation. F| The combined excitatory and inhibitory

area of cortical receptive fields is similar for the two cortical populations ($p=0.71$, two-sided t-test). G| Average modulation depth (distance between the max and min values of the RF) for the two cortical populations. SA1-like cells show a more strongly modulated response to spatial structure than do PC-like cells ($p<0.05$, two-sided t-test), which is consistent with the greater sensitivity of SA1-like neurons to coarse spatial features.

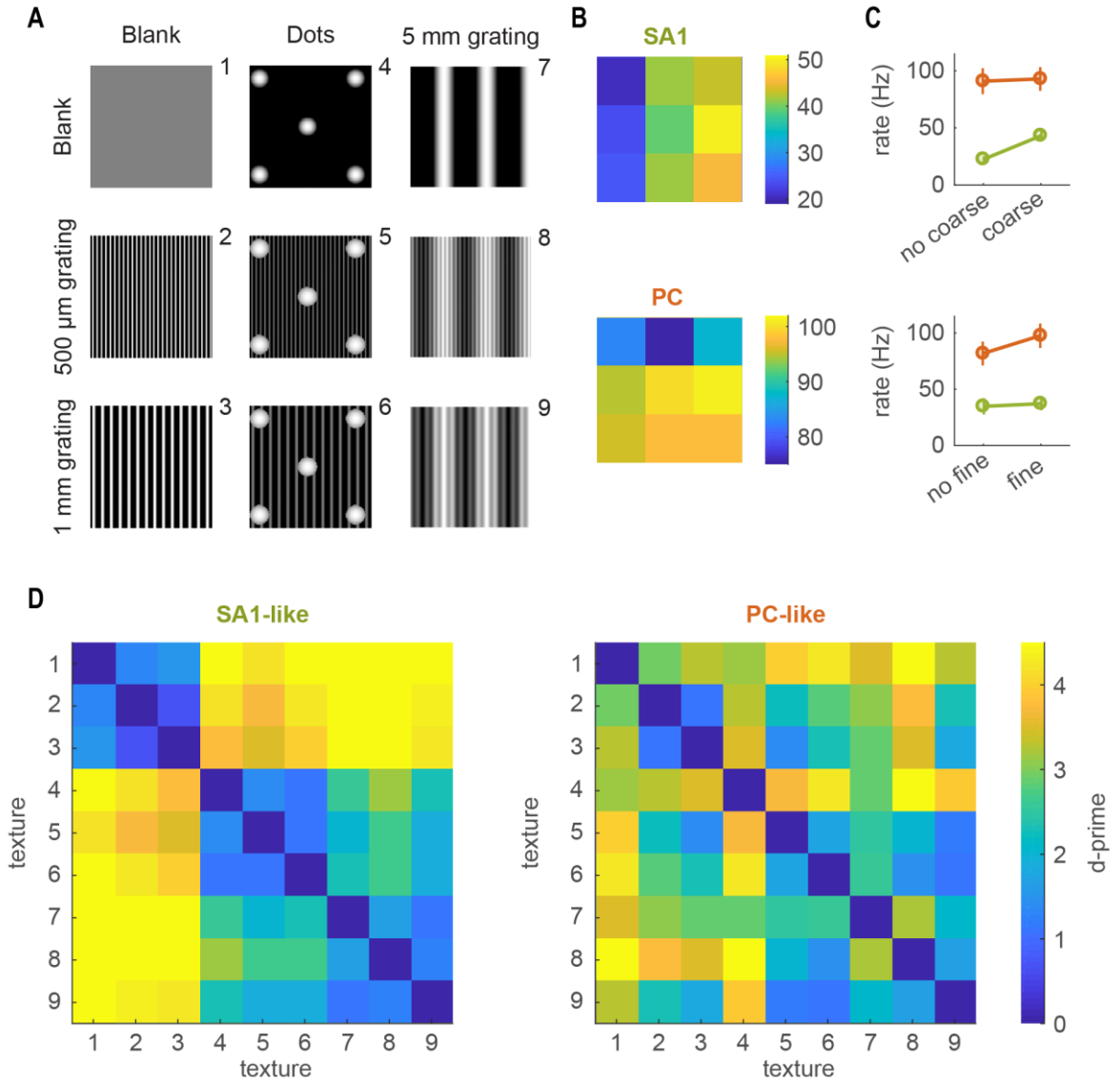

Figure S5. **Coding of texture at different spatial scales.** A| Surface profiles of custom-made 3D-printed textures designed to probe the interaction of coarse and fine features. We parametrically combined three coarse textural features (columns left to right: blank, 7 mm dots, 5 mm grating) with three "fine" ones (rows top to bottom: blank, 0.5 mm grating, 1 mm grating). B| Mean firing rate of SA1-like (SA1 regression coefficient > 0.5, N=53) and PC-like (PC regression coefficient > 0.5, N=23) neurons evoked by all nine textures (arranged as in A). C| Top: Mean firing rate of SA1-like (green) and PC-like (orange) neurons evoked by textures without and with coarse structure: Textures 1-3 do not have coarse structure, textures 4-9 do. Bottom: Mean firing rate of SA1-like (green) and PC-like (orange) neurons evoked by textures without and with fine structure: Textures 1, 4, and 7 do not have fine structure, the others do. Error bars denote the standard errors across cells and textures. SA1-like neurons increase their firing rates when coarse structure is present, while PC-like neurons increase their firing rates when fine structure is present. D| Mean discriminability (d') based on firing rate responses for all possible

pairings of textures, for SA1-like and PC-like neurons. SA1-like responses cannot distinguish surfaces with the same coarse component but differing in the fine component (4 and 6, e.g.), but readily distinguish textures with different coarse components (4 and 8, e.g.). Conversely, PC-like responses cannot distinguish surfaces with the same fine components (6 and 9, e.g.) but readily distinguish surfaces with different fine components (4 and 6, e.g.). Thus, SA1-like neurons are more sensitive to coarse structure than are PC-like neurons, and PC-like neurons are more sensitive to fine structure than are SA1-like neurons.

SUPPORTING TABLE

Velvet [P]	Silk, metallic (silk/metal) [P]	500 micron grating [*]	Upholstery, yellow [P]	Red fabric dots (backing)
Computer paper	Thin corduroy [P]	Upholstery, onyx	Wool, blend [P]	Embossed dots, 5 mm spacing (plastic) [P†]
Microsuede (polyester) [P†]	Organza [P]	Chiffon [P†]	Dots, 7.7 mm spacing [*]	Upholstery, fuzzy
Satin [P†]	Possum fur	1 mm grating [*]	Upholstery, beach mat	Receptive field mapping dots (2nd half)
Sueded cuddle (polyester) [P]	Foam drapery tape [P]	Upholstery, red grating	Upholstery, tan	Upholstery, green
Rabbit fur, long hair	Thick corduroy [P]	Fabric grating, wide spacing	Leather dot pattern	5 mm grating [*]
Vinyl (20 gauge) [P]	Wool/rayon felt [P]	Stretch denim (cotton/Lycra) [P†]	Wrapping paper (bumpy)	Hucktowel (cotton) [P†]
Careerwear flannel (cotton) [P]	Butcher paper	Faux croc skin	Ruffled fabric	Receptive field mapping dots (1st half)
Parchment paper	Nylon (200 denier) [P†]	Upholstery, gridded	Red fabric dots (front)	Embossed dots, 4 mm spacing (plastic) [P†]
Sting ray skin	Denim (cotton) [P]	Silk, crinkled [P]	Dots, 7.7 mm / 500 micron grating overlay [*]	5 mm grating / 1 mm grating overlay [*]
Snowflake fleece fuzz (polyester) [P]	Rabbit fur, short hair	Upholstery, Sunbrella	Dots, 7.7 mm / 1 mm grating overlay [*]	5 mm grating / 500 micron grating overlay [*]
Acrylic (Blank) [*]	Wool gabardine [P]	Lizard skin	Bumpy polyester	

Table S1. **Texture set.** The 59 textures are ordered by their score along the first principal component (predictive of perceived roughness), sorted from low to high by column, then by row. The 24 textures common between the peripheral (6) and cortical experiments are marked with "[P]." Textures that were 3D printed to disambiguate the effects of coarse and fine structure (pictured in Supplementary Figure 11 and used for Figure 5) are marked with "[*]." Textures used to create the spiking rasters in Figure 1 are marked with "[†]."

SUPPORTING REFERENCES

1. Pei Y-C, Denchev P V, Hsiao SS, Craig JC, Bensmaia SJ (2009) Convergence of submodality-specific input onto neurons in primary somatosensory cortex. *J Neurophysiol* 102(3):1843–1853.

2. DiCarlo JJ, Johnson KO, Hsiao SS (1998) Structure of receptive fields in area 3b of primary somatosensory cortex in the alert monkey. *J Neurosci* 18(7):2626–45.

3. Rigotti M, et al. (2013) The importance of mixed selectivity in complex cognitive tasks. *Nature* 497(7451):585–590.

4. Cohen MR, Kohn A (2011) Measuring and interpreting neuronal correlations. *Nat Neurosci* 14(7):811–819.

5. Johnson KO, Phillips JR (1988) A rotating drum stimulator for scanning embossed patterns and textures across the skin. *J Neurosci Methods* 22(3):221–231.

6. Weber AI, et al. (2013) Spatial and temporal codes mediate the tactile perception of natural textures. *Proc Natl Acad Sci U S A* 110(42):17107–17112.